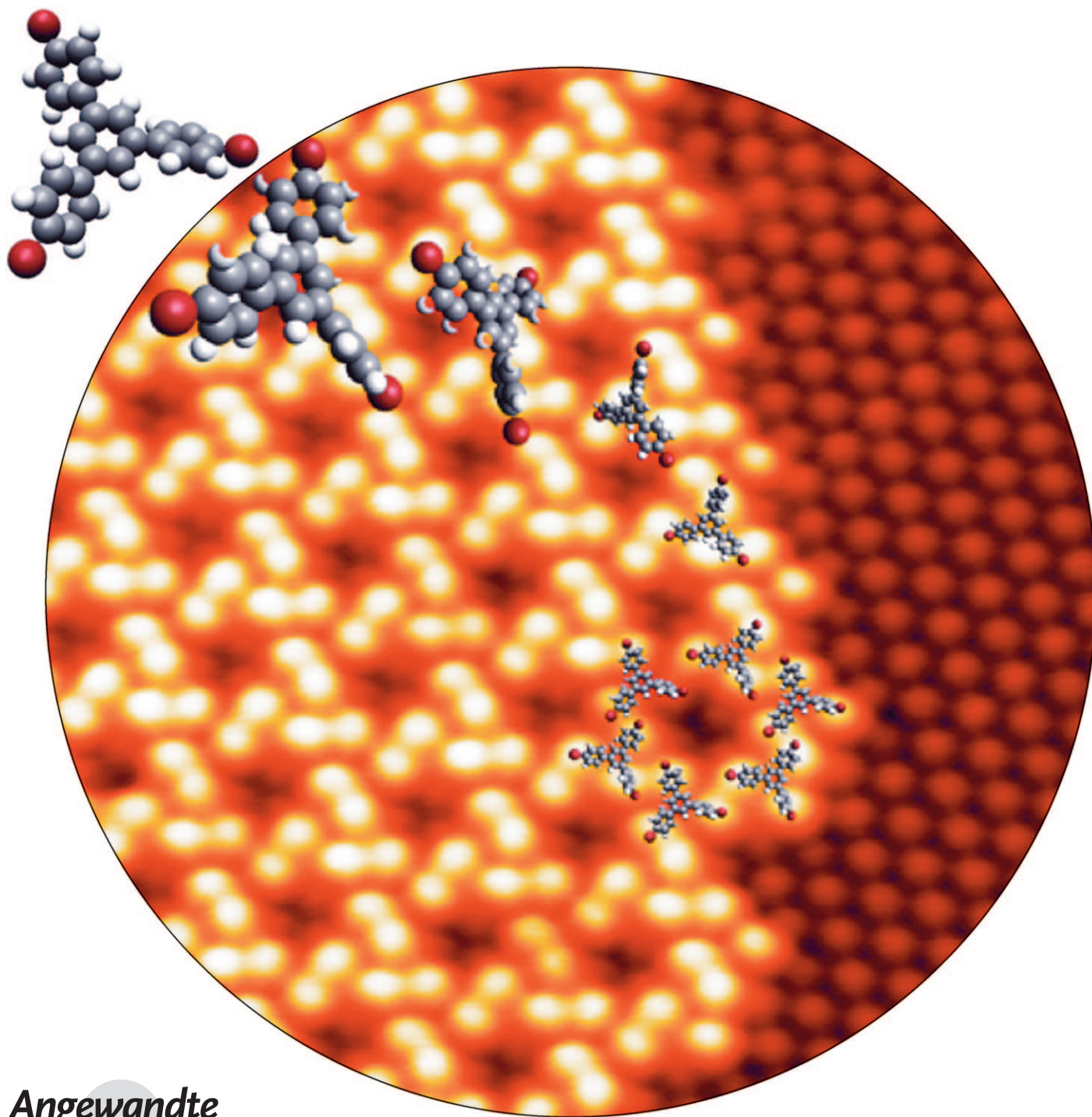# Robust and Open Tailored Supramolecular Networks Controlled by the Template Effect of a Silicon Surface**

*Bulent Baris, Vincent Luzet, Eric Duverger, Philippe Sonnet, Frank Palmino, and Frederic Cherioux**

The development of hybrid organic/inorganic devices with nanoscale features is one of the main challenges for future decades.[1] These objectives require tailored organic molecules with optimal properties (such as for electronics, optics, magnetism, tribology, catalysis, energy conversion, biocompatibility etc.), which can be used as building blocks for the growth of highly ordered supramolecular structures (i.e. with atomic precision).[2] Once the mechanisms that control the self-ordering phenomena are fully understood, the self-assembly and growth processes can create a wide range of nanostructured surfaces from metallic, semiconducting, and molecular materials. Both recent progress in experimental methods capable of investigating and/or manipulating single-atom objects on a surface as well as advances in supramolecular chemistry[3] now allow applications on noble-metal surfaces or highly oriented pyrolitic graphite (HOPG) surfaces.[4–12] Supramolecular engineering is based on the subtle balance between molecule–molecule interactions and molecule–substrate interactions. Nevertheless, the use of semiconducting interfaces remains important for the development of many devices, such as molecular electronics and materials for energy conversion. From an economic point of view, silicon-based surfaces are the best option, because their costs are much lower than the ones for metallic monocrystalline surfaces.[13] Strong molecule–substrate interactions could be rarely avoided so far; they can disrupt the growth of the supramolecular edifice but can also be helpful for nanostructuration by covalent grafting.[14,15] Supramolecular edifices on semiconductors was previously achieved in two ways: 1) tuning molecule–substrate interactions, which can lead to the formation of very small supramolecular assemblies with dimensions smaller than five molecules (i.e. below 10×10 nm^2);[16–19] 2) insertion of doping elements (like Ag) in order to passivate the surface.[20,21] The supramolecular networks can be large (larger than 100×100 nm^2); however, in these cases, the interface never consists of silicon atoms. Herein, we describe in detail the first engineering of a large-scale 2D open supramolecular framework with improved thermal stability up to 400 K on a semiconductor surface, that interacts directly with a silicon atom layer. We describe the engineering of a supramolecular self-assembly on a silicon-based surface. This assembly was achieved by using a Si(111)-B $\sqrt{3} \times \sqrt{3}$R30° reconstruction surface and 1,3,5-tri(4′-bro-mophenyl)benzene (TBB) as molecular building block. The growth of a supramolecular network is controlled by tuning molecule–molecule interactions and molecule–silicon substrate interactions. This robust open honeycomb network controls the growth and serves as a template of a noncompact hexagonal fullerene array from 100 to 370 K. All experimental data were supported by DFT simulations.

To circumvent the problem of silicon surface reactions with π-conjugated molecules, the Si(111)-B $\sqrt{3} \times \sqrt{3}$R30° surface has been used as a substrate. This surface possesses the unique particularity of showing depopulated dangling bonds because of the presence of boron atoms underneath the top silicon layer.[22–24] The distance between two silicon atoms on the surface is 0.66 nm; this surface is obtained by standard ultra-high vacuum (UHV) thermal treatment of commercially available wafers, thus reinforcing its interest for industrial applications. To grow a supramolecular network on a Si(111)-B $\sqrt{3} \times \sqrt{3}$R30° surface, we chose TBB as molecular building block, a molecule with C3 symmetry (similar to the surface symmetry), and with a distance between each substituent that is equal to the distance of two silicon atoms on the surface. The distance between the center of phenyl groups of each arm is 0.68 nm (Figure 1a), while the distance between two bromine atoms is 1.33 nm (Figure 1a).

Figure 1b shows a typical large-scale STM of the TBB/SiB(111) interface for a submonolayer coverage; no isolated molecule is observed. The adsorption of TBB on SiB(111) leads to the formation of very large islands with an area bigger than 800×800 nm^2. These large islands consist of a 2D nanoporous network with very few defects that shows a three-fold symmetry. The step edges of the network are oriented at 120° with respect to one another. A regular molecular network monolayer is observed in the left part of Figure 1c (enlarged picture, Figure S1, in the Supporting Information). The network forms a commensurable structure with a $\sqrt{3} \times \sqrt{3}$ reconstruction (white arrows) of the SiB(111) surface; the periodicity of this network is $3\sqrt{3} \times 3\sqrt{3}$ (black arrows). The open network includes nanopores that are 1.1 nm in width and that contain three small protrusions (white dots denoted S.P. in Figure 1c). The unit cell is formed by two equilateral triangles that each consist of three disjoined protrusions (Figure 1c). The distance measured between the disjoined protrusions, which correspond to the apex of the triangles drawn, is 0.9 nm, whereas the distance between the nearest apexes of two different triangles is 0.6 nm.

Given the dimensions of TBB molecules, three disjoined protrusions (that form a 0.9 nm triangle) are attributed to one TBB molecule and each protrusion corresponds to a bromophenyl arm of TBB. As both the SiB(111) surface and molecular network are observed on the same STM image, the molecular network can be superimposed on the silicon network with a high precision (Figure 2). This hypothesis is strongly supported by the remarkable resolution of STM images, in which the substrate is resolved at the atomic level and the organic network is observed with a submolecular resolution. We establish that the center of TBB molecules is always located between three Si ad-atoms and that the Br—Br axes of TTB molecules are rotated by 30° with respect to Si

[*] B. Baris, V. Luzet, Dr. E. Duverger, Prof. Dr. F. Palmino, Dr. F. Cherioux
FEMTO-ST, Université de Franche-Comté, CNRS, ENSMM
32 Avenue de l'Observatoire, 25044 Besancon cedex (France)
Fax: (+33) 3-8185-3998
E-mail: frederic.cherioux@femto-st.fr

Prof. Dr. P. Sonnet
IS2 M, CNRS UHA
4 rue des Frères Lumière, 68093 Mulhouse (France)

Supporting information for this article is available on the WWW under http://dx.doi.org/10.1002/anie.201100332.
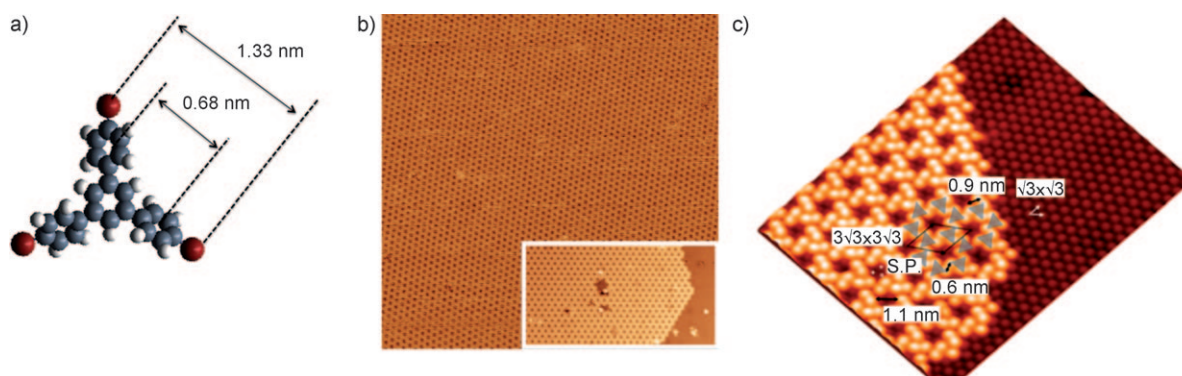
Figure 1. a) CPK (Corey-Pauling-Koltum) model of TBB. b) Large-scale STM image ($V_s = 2.5$ V, $I_t = 0.034$ nA, 120×120 nm^2) of a TBB network on SiB(111) with a TBB step edge island shown in the insert (80×50 nm^2). c) High-resolution close-up of a TBB step edge island on SiB from a perspective view ($V_s = 2.3$ V, $I_t = 0.037$ nA, 15×15 nm^2). Black lines indicate the lattice parameter ($3\sqrt{3} \times 3\sqrt{3}$) of the molecular network. The white dots correspond to the Si ad-atom of the $\sqrt{3} \times \sqrt{3}$ reconstruction.
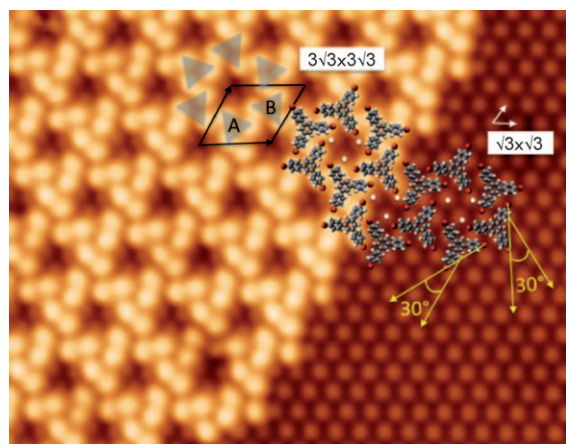

Figure 2. Superimposed model of the TBB network on STM image. The white dots correspond to the Si ad-atom of the $\sqrt{3} \times \sqrt{3}$ reconstruction.

Figure 3. a) Integrated LDOS image of TBB molecular network onto $\sqrt{3} \times \sqrt{3}R30°$ SiB(111), from E_f to $E_f + 2.5$ eV; b) side-view of TBB/SiB(111) optimized at the DFT–GGA level.

ad-atom rows. Nevertheless, the center of the TBB molecule, that is, a phenyl ring, is never observed on the STM images recorded at $+2.5$ V, which is probably due to the absence of density-of-states (DOS) that corresponds to this phenyl ring at this voltage. Owing to the molecular dimension of TBB molecules, the center of bright protrusions (i.e. the bromophenyl substituent) is not located exactly above Si ad-atoms.

These features indicate that there are two molecules per unit cell with two molecular orientations (denoted A and B, Figure 2). Nevertheless, interactions between a single molecule and SiB(111) are weak because no isolated molecules are observed in the 100–400 K temperature range. Molecule orientations and the TBB molecular dimension explain the formation of nanopores. We can now attribute the three small protrusions observed in the nanopores (white dots in Figure 2, enlarged picture, Figure S2, in the Supporting Information) to three Si ad-atoms of the uncovered $\sqrt{3} \times \sqrt{3}$ reconstruction. DFT calculations (VASP code) were performed using the adsorption model proposed in Figure 2 (see the Supporting Information). The local DOS (LDOS) image of the TBB network was realized at $E_f - E_f + 2.5$ eV (Figure 3, enlarged picture, Figure S3, in the Supporting Information). We
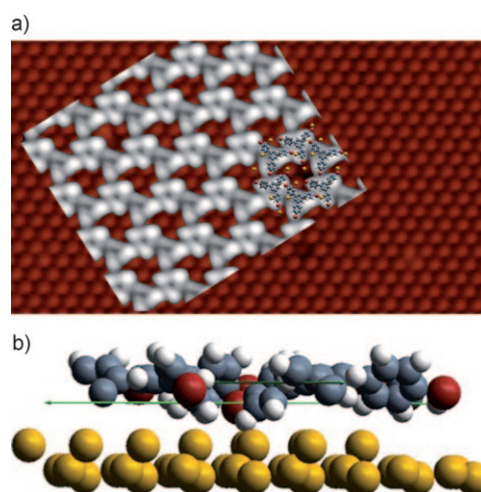
observe three protuberances per TBB molecule associated with the phenyl arms; the LDOS image is consistent with the experimental STM images and confirms the proposed molecular TBB network on SiB.

The molecular network geometry does not depend on the TBB–surface interaction alone, for example the TBB–HOPG interface shows a compact network,[25] but also on the molecule–molecule interactions, like halogen–halogen interactions between TBB molecules on Cu(111).[26] In our case, however, halogen–halogen interactions are impossible because the bromine atoms do not point towards one another. A close examination of the STM images in the empty states shows that there is shared electronic DOS between the bromophenyl arms of neighboring molecules that show an interaction (see Figure S4 in the Supporting Information). Molecule–molecule interactions were simulated by DFT, giving a value of 0.16 eV, which can be attributed to a weak repulsive π–π interaction. Moreover, deformation energies of the molecules absorbed in the supramolecular network are slightly higher than in the gas phase, thus increasing the

energy by 0.58 eV. This effect leads to a small bending of a bromophenyl substituent through the SiB(111) surface, as shown in Figure 3b, thus explaining the nonequivalent brightness of protrusions associated with a TBB molecule in LDOS integrated images (Figure 3a) and experimental STM images (Figure 1b,c). Nevertheless, despite these two unfavorable interactions, the interaction energy between supramolecular networks and the surface was calculated by DFT and is -0.33 eV. The total SiB template effect is -0.33 eV -0.58 eV -0.16 eV $= -1.07$ eV, with a calculated TBB–SiB distance of 0.41 nm. The substrate template effect stems from the matching of the geometrical parameters of the surface and the TBB molecules (size and symmetry). The molecules are adsorbed in such a way that each bromophenyl ring interacts with an electron-poor silicon ad-atom. Thus, it is a strong template effect that overcomes the constrained molecules and repulsive molecule–molecule interactions in the 2D network and finally stabilizes the supramolecular network on the SiB substrate. A similar effect was observed by Feringa and co-workers in the case of polymorphism of Schiff base derivatives on a Au(111) surface.[27]

Many works have discussed the trapping of fullerenes in molecular nanoporous networks on noble-metal surfaces[10,17,18,28–32] or on semiconductor surfaces.[33] As the 1.1 nm width of the pores, that is the largest distance between two bright protrusions, matches the covalent diameter of C_{60} (0.8 nm), the filling of each TBB nanopore by a single C_{60} was investigated.

Figure 4 shows STM images of C_{60} molecules adsorbed onto nanopores of a TBB molecular network with an atomic resolution of the SiB(111) substrate and submolecular resolution of the organic network and C_{60} recorded at 110 K. Figure 4a shows the C_{60}–TBB–SiB(111) interface for a very low C_{60} coverage (below 0.1 monolayer (ML)). No protrusion is observed on the SiB(111) substrate and over the TBB molecules. The measured diameter of the protrusions (2 nm) observed on STM images is compatible with the van der Waals C_{60} diameter observed by STM on other systems.[31] Therefore, each protrusion is attributed to a single C_{60} molecule adsorbed above the nanoporous TBB network. For a 0.5 ML coverage of C_{60} (Figure 4b), less than 1% of C_{60} is isolated and local compact networks are observed. For approximately 1 ML (Figure 4c), a quasi-complete C_{60} network is obtained with a perfect hexagonal $3\sqrt{3} \times 3\sqrt{3}$ periodicity, close to the TBB network periodicity (Figure 2). The protrusions that are associated with C_{60} molecules are only seen within the pores of the TBB network and not on the bare SiB(111) substrate or directly above the TBB molecules within the network. In order to confirm that a protrusion corresponds to a single adsorbed C_{60}, DFT calculations were performed. The LDOS image of the TBB network with C_{60} was calculated at $E_f + 2.5$ eV and is consistent with experimental STM images (Figure 5).
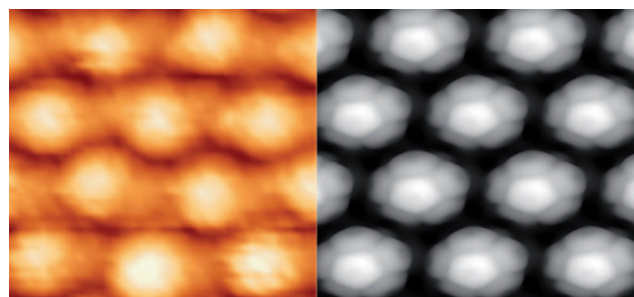

Figure 5. STM image (left, 6×6 nm^2, $V_s = 2.5$ V, $I_t = 0.034$ nA) and integrated LDOS (right, 6×6 nm^2, from E_f to $E_f + 2.5$ eV) of a C_{60} monolayer adsorbed onto a TBB/SiB(111) network.
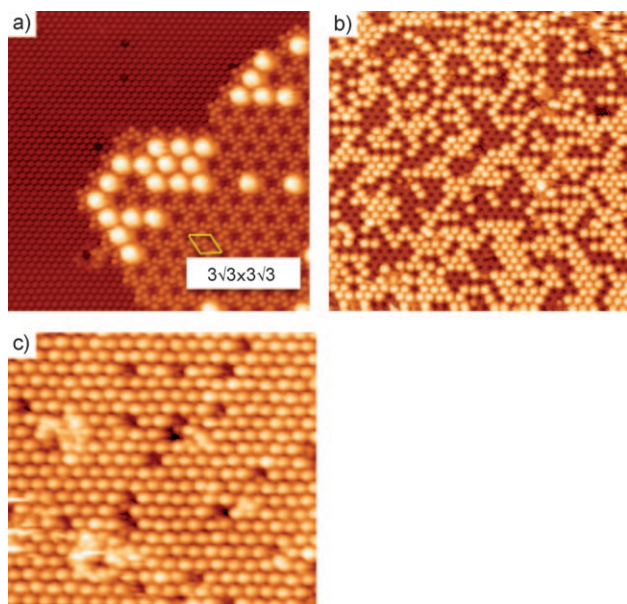

Figure 4. STM images of C_{60} on TBB network deposited onto $\sqrt{3} \times \sqrt{3}$R30° SiB(111); a) 30×30 nm^2, $V_s = 2.7$ V, $I_t = 0.015$ nA, 0.1 ML; b) 70×70 nm^2, $V_s = 1.9$ V, $I_t = 0.034$ nA, 0.5 ML; c) 45×49 nm^2, $V_s = 2.5$ V, $I_t = 0.006$ nA, 1.0 ML.

According to the theoretical calculations, the interaction energy of C_{60} with the TBB–SiB(111) network is -0.35 eV with a C_{60}–SiB surface distance of 0.59 nm. This value is consistent with the apparent height determined by Fasel and co-workers in the case of C_{60} on corannulene/Cu(110) (i.e. 0.45 ± 0.2 nm).[31] C_{60} is a strongly electron-withdrawing molecule that interacts with the electron-rich bromophenyl arms located within the nanopores. This effect explains the specific C_{60} adsorption above the nanopores of the organic network.

We report the formation of a large-scale 2D open supramolecular network on a silicon surface with a thermal stability up to 400 K. This framework is achieved thanks to the combination of repulsive molecule–molecule interactions and attractive molecule–surface interactions. Deposition of C_{60} molecules onto this robust open network leads to the growth of a noncompact hexagonal fullerene array at room temperature. The use of SiB(111) paves a new route towards a class of robust, commensurable, and polyfunctional organic networks adsorbed on a silicon surface.

Zuschriften

[1] C. Joachim, J. K. Gimzewski, A. Aviram, *Nature* **2000**, *408*, 541–548.

[2] M. Bowker, P. R. Davies in *Scanning Tunneling Microscopy in Surface Science, Nanoscience and Catalysis*, Wiley-VCH, Weinheim, **2010**.

[3] J.-M Lehn in *Supramolecular Chemistry: Concepts and Perspectives*, Wiley-VCH, Weinheim, **1995**.

[4] L. Bartels, *Nat. Chem.* **2010**, *2*, 87–95.

[5] J. V. Barth, *Surf. Sci.* **2009**, *603*, 1533–1541.

[6] L. Grill, M. Dyer, L. Lafferentz, M. Persson, M. V. Peters, S. Hecht, *Nat. Nanotechnol.* **2007**, *2*, 687–691.

[7] J. V. Barth, G. Constantini, K. Kern, *Nature* **2005**, *437*, 671–679.

[8] J. A. A. W. Elemans, S. Lei, S. De Feyter, *Angew. Chem.* **2009**, *121*, 7434–7469; *Angew. Chem. Int. Ed.* **2009**, *48*, 7298–7332.

[9] K. Müllen, J. P. Rabe, *Acc. Chem. Res.* **2008**, *41*, 511–520.

[10] B. Calmettes, S. Nagarajan, A. Gourdon, M. Abel, L. Porte, R. Coratger, *Angew. Chem.* **2008**, *120*, 7102–7106; *Angew. Chem. Int. Ed.* **2008**, *47*, 6994–6998.

[11] J. M. Macleod, O. Ivasenko, C. Y. Fu, T. Taerum, F. Rosei, D. F. Perepichka, *J. Am. Chem. Soc.* **2009**, *131*, 16844–16850.

[12] O. Guillermet, E. Niemi, S. Nagarajan, A. Gourdon, X. Bouju, D. Martrou, A. Gourdon, S. Gauthier, *Angew. Chem.* **2009**, *121*, 2004–2007; *Angew. Chem. Int. Ed.* **2009**, *48*, 1970–1973.

[13] A Au(111) single crystal costs 1200$ and a piece of silicon wafer 0.01$.

[14] G. P. Lopinski, D. D. M. Wayner, R. A. Wolkow, *Nature* **2000**, *406*, 48–51.

[15] M. Z. Hossain, H. S. Kato, M. Kawai, *J. Am. Chem. Soc.* **2008**, *130*, 11518–11523.

[16] K. R. Harikumar, L. Leung, I. R. McNab, J. C. Polanyi, H. P. Lin, W. A. Hofer, *Nat. Chem.* **2009**, *1*, 712–716.

[17] R. Hamers, S. K. Coulter, M. D. Ellison, J. S. Hovis, D. F. Padowitz, M. P. Schwartz, C. M. Greenlief, J. N. Russell, *Acc. Chem. Res.* **2000**, *33*, 617–624.

[18] P. A. Sloan, R. E. Palmer, *Nature* **2005**, *434*, 367–371.

[19] Y. Makoudi, M. Arab, F. Palmino, E. Duverger, C. Ramseyer, F. Picaud, F. Cherioux, *Angew. Chem.* **2007**, *119*, 9447–9450; *Angew. Chem. Int. Ed.* **2007**, *46*, 9287–9290.

[20] J. A. Theobald, N. S. Oxtoby, N. R. Champness, P. H. Beton, T. J. S. Dennis, *Langmuir* **2005**, *21*, 2038–2041.

[21] J. A. Theobald, N. S. Oxtoby, M. A. Phillips, N. R. Champness, P. H. Beton, *Nature* **2003**, *424*, 1029–1031.

[22] I.-W. Lyo, E. Kaxiras, P. Avouris, *Phys. Rev. Lett.* **1989**, *63*, 1261–1264.

[23] Y. Makoudi, F. Palmino, E. Duverger, M. Arab, F. Cherioux, C. Ramseyer, B. Therrien, M. J.-L. Tschan, G. Süss-Fink, *Phys. Rev. Lett.* **2008**, *100*, 076405.

[24] Y. Makoudi, M. Arab, F. Palmino, E. Duverger, F. Cherioux, *J. Am. Chem. Soc.* **2008**, *130*, 6670–6671.

[25] R. Gutzler, H. Walch, G. Eder, S. Kloft, W. M. Heckl, M. Lackinger, *Chem. Commun.* **2009**, 4456–4458.

[26] H. Walch, R. Gutzler, T. Sirtl, G. Eder, M. Lackinger, *J. Phys. Chem. C* **2010**, *114*, 12604–12609.

[27] T. Kudernac, N. Sändig, T. Fernandez Landaluce, B. J. van Wees, P. Rudolf, N. Katsonis, F. Zerbetto, B. L. Feringa, *J. Am. Chem. Soc.* **2009**, *131*, 15655–15659.

[28] L. Piot, F. Silly, L. Tortech, Y. Nicolas, P. Blanchard, J. Roncali, D. Fichou, *J. Am. Chem. Soc.* **2009**, *131*, 12864–12865.

[29] S. Yoshimoto, Y. Honda, O. Ito, K. Itaya, *J. Am. Chem. Soc.* **2008**, *130*, 1085–1092.

[30] D. Bonifazi, A. Kiebele, M. Stohr, F. Cheng, T. Jung, F. Diederich, H. Spillmann, *Adv. Funct. Mater.* **2007**, *17*, 1051–1062.

[31] W. Xiao, D. Passerone, P. Ruffieux, K. Aït-Mansour, O. Gröning, E. Tosatti, R. Fasel, *J. Am. Chem. Soc.* **2008**, *130*, 4767–4771.

[32] M. O. Blunt, J. C. Russell, M. d. C. Gimenez-Lopez, N. Taleb, X. Lin, M. Schröder, N. R. Champness, P. H. Beton, *Nat. Chem.* **2011**, *3*, 74–78.

[33] P. J. Moriarty, *Surf. Sci. Rep.* **2010**, *65*, 175–227.